ELSEVIER

Polymer 42 (2001) 7455–7460

polymer

www.elsevier.nl/locate/polymer

Effect of hybrid layers with different silane coupling agents on impact response of glass fabric reinforced vinylester matrix composites

Jang-Kyo Kim[a,*], Man-Lung Sham[a], Min-Seok Sohn[a,1], Hiroyuki Hamada[b]

[a]*Department of Mechanical Engineering, Hong Kong University of Science and Technology, Clear Water Bay, Kowloon, Hong Kong*
[b]*Department of Polymer Science and Engineering, Faculty of Textile Science, Kyoto Institute of Technology, Matsugasaki, Sakyo, Kyoto 606, Japan*

Received 15 November 2000; received in revised form 23 January 2001; accepted 8 February 2001

Abstract

The damage resistance of woven glass reinforced vinylester matrix composites after low-velocity impact is evaluated. The composites have a hybrid laminate structure, consisting of fabric layers treated with different silane coupling agents. It is shown that the extent of damage and the residual mechanical properties as measured in compression-after-impact (CAI) tests are affected strongly by the combination of hybrid layers and the position of individual layers with particular silane treatment relative to the impact front surface. There is strong correlation between the mode II interlaminar fracture toughness and the impact damage performance of hybrid composites. © 2001 Published by Elsevier Science Ltd.

Keywords: E-glass woven-fabric laminates; Hybrid layer; Silane coupling agent

1. Introduction

The significance of using hybrid fibre composites is to optimize useful properties that cannot be achieved with one type of fibre. Driving forces for employing two or more types of fibre with a common matrix material are twofold [1–5]: one is to reduce the cost of expensive carbon fibre reinforced plastic (CFRP) composites by incorporating cheaper glass fibres, and the other is to utilise the inherent ductility of aramid, glass or ultra-high molecular weight polyethylene (UHMPE) fibres that can counterbalance the brittleness of typical CFRP composites. The poor impact performance of CFRPs has been a major issue from the design viewpoint, and the hybrid fibre concept has been widely used to enhance the impact damage resistance [6,7].

Significant research efforts have been made to understand the effects of type of fibre employed, method of fibre mixture and stacking sequence on the structural and mechanical performance of hybrid composites. Hybridizing carbon layers with less number of layers of UHMPE fibre resulted in a substantial improvement in impact damage performance with negligible reductions in tensile and flexural strengths [8]. The stacking sequence played a critical role in controlling the deformation and damage processes under low velocity impact [4,5,9–11]. The laminates with asymmetric stacking sequences tended to outperform those with symmetric stacking sequence. The laminates with brittle layers in the front (i.e. compressive side) and flexible layers in the back surface (i.e. tensile side) of impact (Fig. 1(a)) offered a better impact damage resistance than the other combinations of layer and stacking sequence (Fig. 1(b)). This is because the brittle layers absorb effectively the majority of incident impact energy by means of extensive damage processes, such as fracture and delamination, and the rest of impact energy is dissipated by the flexible layers mainly through inelastic deformation. A similar conclusion was also drawn in high velocity impact of carbon/UHMPE hybrid composites that the highest impact energy values for penetration was obtained by positioning the UHMPE layers in the back surface of impact [10].

Apart from stacking sequence, the fibre–matrix interface adhesion is another important factor that controls the impact performance of hybrid composites. A strong adhesion is necessary to achieve efficient stress transfer between the fibre and matrix and thus high composite strength and stiffness, but is not always favourable for high damage resistance and fracture performance [12]. There is inevitable compromise between the high strength/stiffness and the high ductility/fracture resistance as these mechanical properties are influenced by the fibre–matrix interface adhesion

---

* Corresponding author. Tel.: +852-2358-7207; fax: +852-2358-1543.
E-mail address: mejkkim@ust.hk (J.-K. Kim).

[1] On leave from Department of Mechanical and Materials Engineering, University of Western Australia, Nedland, WA 6907, Australia.

0032-3861/01/$ - see front matter © 2001 Published by Elsevier Science Ltd.
PII: S0032-3861(01)00246-4

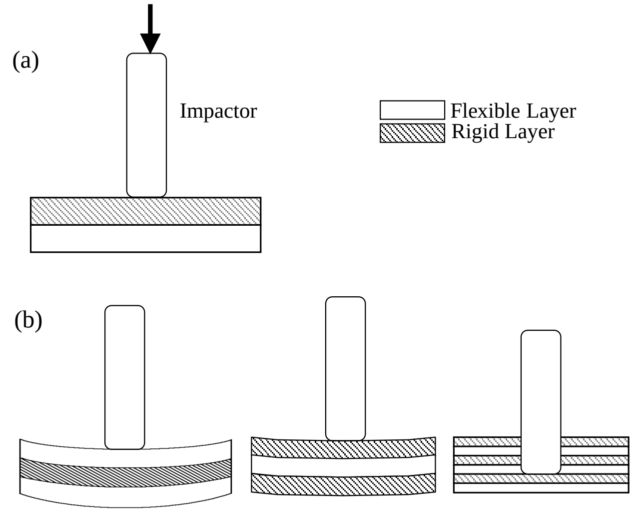

Fig. 1. Schematic drawings of deformation modes in hybrid laminate composites with different stacking sequences upon impact loading: (a) asymmetric configuration; (b) symmetric configuration.

in a rather opposite way. Following our previous studies on hybrid composites containing layers with glass fibres treated with different silane coupling agents [13], the present paper reports the damage resistance of hybrid composites after low-energy impact loading. In light of the brief review discussed above, the combining effects of interface adhesion and stacking sequence are specifically studied on the residual properties after low energy impact damage.

2. Experiments

2.1. Materials and fabrication of composite

All materials used in this study, including fibres, matrix materials and coupling agents, were essentially the same as those reported previously [14,15]. The woven E-glass fabrics contained 44 (warp) × 34 (weft) strands per $2.5 \times 2.5\ \mathrm{cm}^2$ unit area. Each strand consisted of 400 filaments of 9 μm in diameter. The matrix material was an unsaturated vinylester resin (Ripoxy R806), and was cross-linked with 0.7 wt% methyl ethyl ketone peroxide (MEKP). Two different types of coupling agents were used: γ-methacryloxypropyltrimethoxysilane (γ-MPS) and γ-glycidoxypropyltrimethoxysilane (γ-GPS). Five different combinations of the two coupling agents were formulated: 0.01 wt% (M0.01), 0.4 wt% (M0.4), 1.0 wt% (M1.0), methanol washed 0.4 wt% (MW0.4) γ-MPS and 0.4 wt% γ-GPS (E0.4). The hand lay-up technique was employed to produce 20-ply laminates with all warp strands being oriented in the same direction. Four different laminates with asymmetric lay-up sequences,

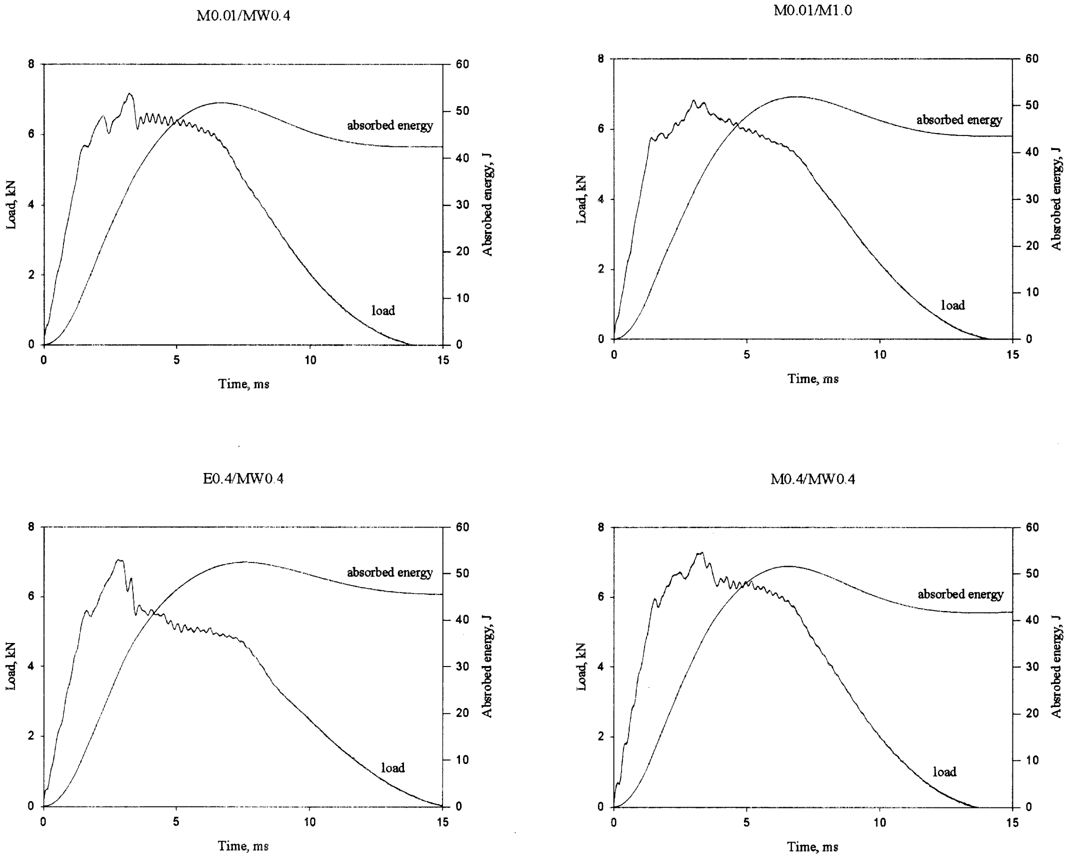

Fig. 2. Load–time and energy–time curves of hybrid laminates under 50 J impact.

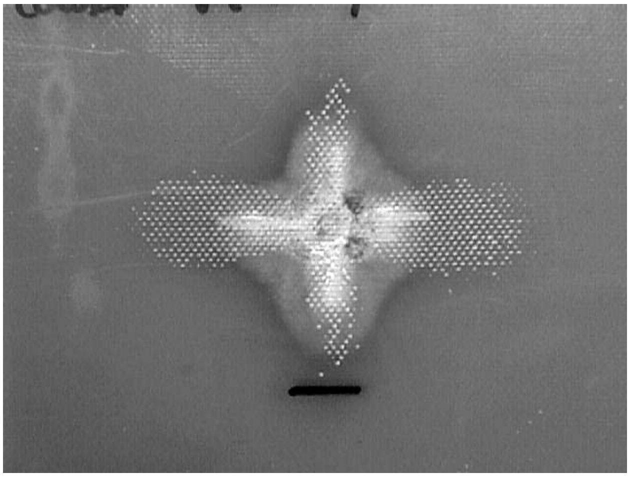

Front face

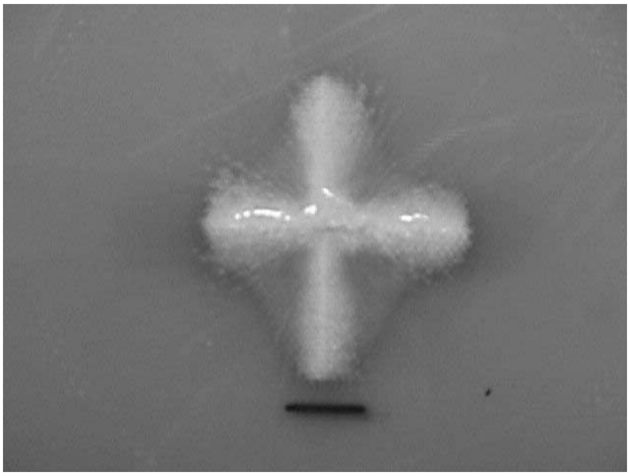

Back face

Fig. 3. Typical damage modes in the (a) front and (b) back impact surfaces of hybrid laminates (M0.01$_{10}$/MW0.4$_{10}$) impacted at 50 J.

designated as [M0.01$_{10}$/MW0.4$_{10}$], [M0.01$_{10}$/M1.0$_{10}$], [E0.4$_{10}$/MW0.4$_{10}$] and [M0.4$_{10}$/MW0.4$_{10}$], were prepared, which were subsequently cured at room temperature for 48 h, followed by post-cure at 80°C for 3 h and at 150°C for 2 h in an oven. The nominal thickness of laminate plate was 4 mm and the fibre volume fraction was about 0.426. The hybrid laminates were cut into square specimens of $100 \times 100\ \mathrm{mm}^2$.

2.2. Specimens and tests

Low-velocity impact tests were conducted on an instrumented impact test machine (GRC Dynatup 8250). The specimen edges were firmly fixed between two circular rings having a test window of 76 mm in diameter. The impact energy level varied in the range of 20–50 J, adjusted by the height of a hemi-spherical impactor of 12.7 mm in radius, relative to the specimen. The load–displacement records were obtained directly from the data acquisition system. Impact-induced damage areas in the front and back surfaces of specimens were measured using an image analysis technique. The compression-after-impact (CAI) tests were conducted to evaluate the damage tolerance of the hybrid composites using a fixture (Boeing Specification Standard BSS 7260). The simply supported boundary conditions on the side edges were included in the fixture to prevent out-of-plane buckling of the specimens. All CAI tests were conducted on a computerized universal testing machine in the weft direction at a crosshead speed of 0.5 mm/min at room temperature. The compressive strengths of undamaged specimens were also measured for comparison.

3. Results and discussions

Typical impact load and energy curves are shown as a function of time generated at incidental impact energy of 50 J in Fig. 2. All curves for laminates with different fibre surface treatments looked basically similar. The characteristic load points, P_{i} (incipient damage load) and P_{m} (maximum load), were clearly noted. The incipient damage load, mainly due to delamination or debond initiation at the initial stage of impact, was identified by the first sudden load drop after the linear increase in load. The maximum or peak load corresponds to the load that the laminate can sustain before subjecting to major damage. Both the P_{i} and P_{m} values obtained from the four different hybrid laminates were approximately the same in the range from 5.5 to 6 kN and from 6.8 to 7.2 kN, respectively. This indicates that the in-plane mechanical properties determined the characteristic impact load–displacement records, while the laminar interface properties affected by the layers of different silane coupling agents did not play a significant role.

Damage of the impacted laminates was characterised using a stereo microscope with the aid of high intensity transmitted and reflected light [14]. Fig. 3 illustrates typical damage modes of the front and back surfaces of the laminate (M0.01$_{10}$/MW0.4$_{10}$) after impact loading at an energy of 50 J. Extensive fibre breakages were seen in the front face of the laminates, where the impactor was directly contacted. Meanwhile, substantial delamination, matrix cracking and fibre fractures were observed in the back face. These damage modes are essentially similar to those reported for the non-hybrid laminates [14,15]. Four different regions were identified corresponding to different damage modes in the back face of laminates, namely (i) major delamination, matrix cracking and transverse fibre fracture; (ii) extensive macro interface debond cracks both in the warp and weft directions; (iii) microscopic interface cracks in the warp direction; (iv) microscopic interface cracks in the weft direction.

The major damage area in the central area of specimens

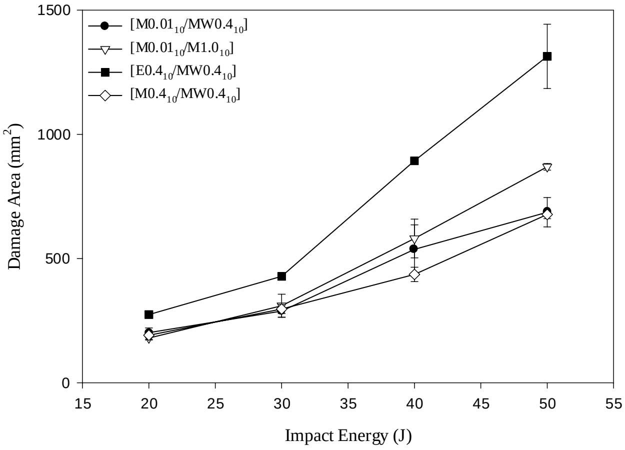

Fig. 4. Damage area as a function of impact energy.

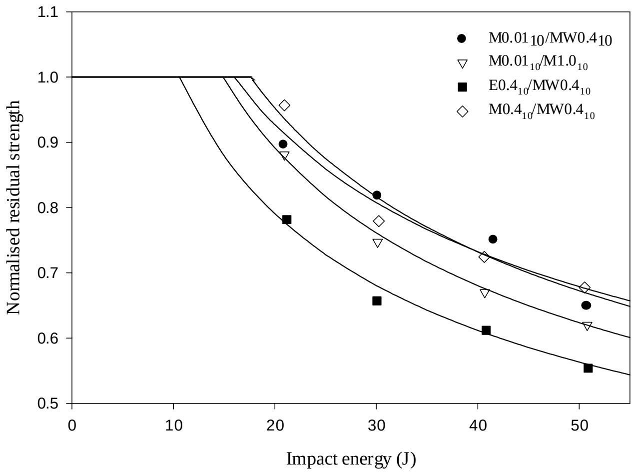

Fig. 5. Normalized residual CAI strength, σ_r/σ_0, plotted as a function of impact energy, U.

was measured and plotted in Fig. 4. The laminate with ($E0.4_{10}/MW0.4_{10}$) layers exhibited the largest damage area for all impact energy studied, the difference in damage area increasing with increasing impact energy. While the other three hybrid laminates showed similar damage performance, the laminates ($M0.01_{10}/MW0.4_{10}$) and ($M0.4_{10}/MW0.4_{10}$) were marginally more resistant to damage than the laminate with ($M0.01_{10}/M1.0_{10}$) layers, especially at high impact energy levels. The residual compressive strengths were measured after impact damage, and the normalized values are plotted in Fig. 5. By employing a simple model of residual CAI strength proposed previously [16],

$$\frac{\sigma_r}{\sigma_0} = \left(\frac{U_0}{U}\right)^{\beta}, \tag{1}$$

two damage parameters, U_0 and β, were obtained [14,15]. U_0 is the threshold impact energy that the material can withstand without any strength degradation, whereas β is the threshold coefficient corresponding to the gradient of strength degradation with absorbed energy. σ_0 and σ_r are the original strength without damage and the residual CAI strength after impact energy, U, respectively. The damage parameters were determined from the least-square fitted log–log plots of the experimental data shown in Fig. 5:

$$\log \sigma_r = \log \sigma_0 + \beta(\log U_0 - \log U). \tag{2}$$

Similarly, the threshold damage area, C_0, below which no strength reduction takes place and the corresponding threshold coefficient, α, were also determined using the equation:

$$\frac{\sigma_r}{\sigma_0} = \left(\frac{C_0}{C}\right)^{\alpha}. \tag{3}$$

These damage parameters thereby obtained are summarized and compared with those for non-hybrid laminates taken from the previous study [14], in Table 1. It is noted that the threshold impact energy was lower and the threshold damage area was larger in the order of the laminates ($E0.4_{10}/MW0.4_{10}$), ($M0.01_{10}/M1.0_{10}$), ($M0.01_{10}/MW0.4_{10}$) and ($M0.4_{10}/MW0.4_{10}$), indicating that the damage resistance and damage tolerance are lower in the same order. Meanwhile, the difference threshold coefficients, α and β, were marginal between the different hybrid laminates, reflecting similar rates of strength reduction with the increases in impact energy and damage area. The hybrid laminates had threshold energy values generally lower and the threshold damage area higher than the non-hybrid laminates, indicating the inferior impact damage resistance and damage tolerance for the hybrid laminates.

An attempt was made to correlate the above findings

Table 1

Impact damage parameters, including the threshold impact energy, U_0, threshold damage area, C_0, and threshold coefficients, β and α, for non-hybrid and hybrid laminate composites

Non-hybrid	Impact parameters		Hybrid	Impact parameters			
	U_0 (J)	β		U_0 (J)	β	C_0 (mm^2)	α
M0.01	16.3	0.34	$M0.01_{10}/MW0.4_{10}$	16.0	0.34	128.9	0.24
M0.4	19.0	0.38	$M0.01_{10}/M1.0_{10}$	14.9	0.39	92.5	0.22
M1.0	22.6	0.32	$E0.4_{10}/MW0.4_{10}$	10.6	0.37	67.1	0.20
MW0.4	17.5	0.30	$M0.4_{10}/MW0.4_{10}$	17.6	0.38	139.8	0.27
E0.4	15.9	0.25					

Table 2
Quasi-static mode I and II interlaminar fracture toughness of non-hybrid and hybrid laminate composites

Non-hybrid laminates	Interlaminar fracture toughness (kJ/m^2)		Hybrid laminates	Interlaminar fracture toughness (kJ/m^2)	
	Mode I	Mode II		Mode I	Mode II
M0.01	0.74	0.98	M0.01$_{10}$/MW0.4$_{10}$	0.57	2.03
M0.4	0.4	2.10	M0.01$_{10}$/M1.0$_{10}$	0.65	1.94
M1.0	0.31	2.47	E0.4$_{10}$/MW0.4$_{10}$	0.45	1.59
MW0.4	0.42	2.31	M0.4$_{10}$/MW0.4$_{10}$	0.58	2.43
E0.4	0.32	1.75			

with other mechanical properties of the laminates. It was found that a high impact damage resistance and damage tolerance corresponds approximately to high interlaminar fracture toughness, especially in mode II shear. The interlaminar fracture toughness values measured in our previous studies [17] are summarized in Table 2, and the correlation with impact damage performance is illustrated in Fig. 6. For all hybrid laminates studied, the normalized CAI strength closely matched with the mode II interlaminar fracture toughness, G_{IIC} (Fig. 6(a)). Indeed, there are linear relationships between the threshold parameters, U_0 and C_0, and G_{IIC} of the laminates (Fig. 6(b)). The above correlation further confirms that the mode II interlaminar fracture toughness is a good indicator of impact damage resistance of a laminate [18,19]. The ductility of matrix material and the interface adhesion have been shown to be the two predominant factors controlling the interlaminar fracture toughness of composites, which in turn influence the impact performance.

4. Concluding remarks

Hybrid laminate composites were fabricated with fabric layers of different fibre surface treatments. The low-velocity impact tests were performed and the residual CAI strengths were measured to evaluate the damage resistance and damage tolerance of the hybrid laminates. The following can be highlighted from this study:

1. The damage modes of hybrid laminates are similar to those observed in non-hybrid laminates as damages modes are determined mainly by the in-plane mechanical properties of laminates.
2. The impact damage resistance and damage tolerance are lower in the order of the laminates (E0.4$_{10}$/MW0.4$_{10}$), (M0.01$_{10}$/M1.0$_{10}$), (M0.01$_{10}$/MW0.4$_{10}$) and (M0.4$_{10}$/MW0.4$_{10}$). Strong correlations are established between the threshold impact energy, the threshold damage area and the mode II interlaminar fracture toughness of the hybrid laminates. The implication is that the impact performance of hybrid laminates can be improved by selecting combinations of layers with high mode II interlaminar fracture toughness values.
3. The impact performance of hybrid laminates is in general inferior to that of non-hybrid laminates, despite the previous finding of higher tensile and flexural strengths of hybrid laminates containing layers treated with certain combinations of silane coupling agent.

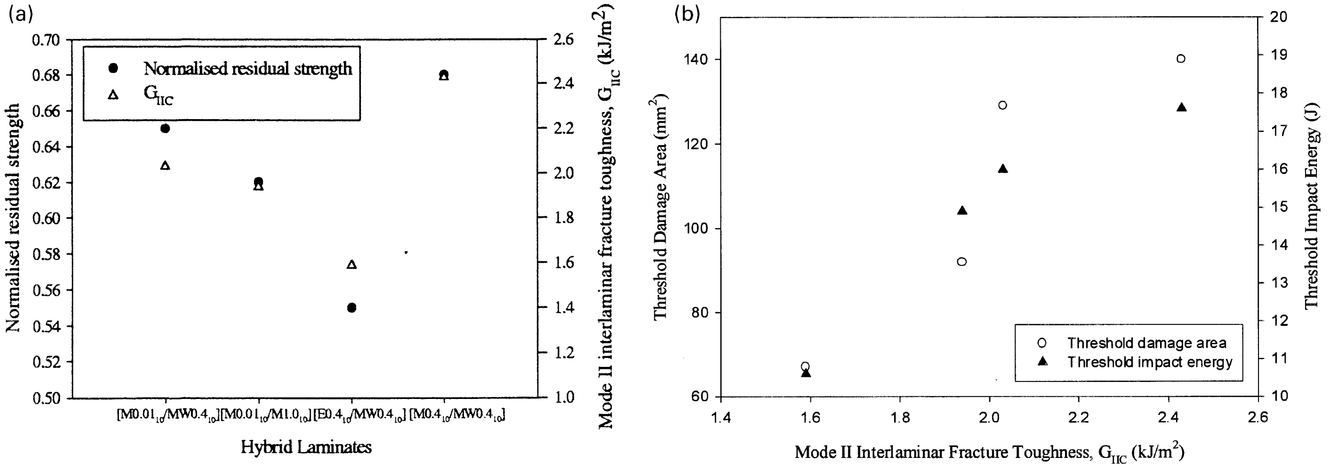

Fig. 6. (a) Correlation between the residual CAI strength, σ_r, and mode II interlaminar fracture toughness, G_{IIC}, for different hybrid laminates. (b) Correlations between the threshold damage area, C_0, threshold impact energy, U_0, and mode II interlaminar fracture toughness, G_{IIC}.

Acknowledgements

The author (JKK) wishes to thank the Research Grants Council for the continuing support of this project through the grant HKUST817/96E. Specimen preparation and part of experiments were carried out while MLS was seconded to Kyoto Institute of Technology, Kyoto, Japan. The technical support provided by the Material Characterization and Preparation Facilities (MCPF) and the Advanced Engineering Materials Facilities (AEMF) at HKUST is also gratefully acknowledged.

References

[1] Harris B, Bunsell AR. Impact properties of glass fibre/carbon hybrid composites. Composites 1975;6:197–201.

[2] Dorey G, Sidey GR, Hutchings J. Impact properties of carbon/Kevlar 49 fibre hybrid composites. Composites 1978;9:25–32.

[3] Bader MG, Manders PW. The strength of glass/carbon fibre composites. Part I. Failure strain enhancement and failure mode. J Mater Sci 1981;16:2233–45.

[4] Marom G, Drukker E, Weinberg A, Banbaji J. Impact behaviour of carbon/Kevlar hybrid composites. Composites 1986;17:150–3.

[5] Jang JS, Moon SI. Impact behaviour of carbon fibre ultra-high modulus polyethylene fibre hybrid composites. Polym Compos 1995;16:325–9.

[6] Kim JK. Methods for improving impact damage resistance of CFRPs. Key Engng Mater 1998;141–3:149–68.

[7] Kim JK, Sham ML. Impact and delamination failure of woven fabric composites. Compos Sci Technol 2000;60:745–61.

[8] Peijs AAJM, Venderbosch RW, Lemstra PJ. Hybrid composites based on polyethylene and carbon fibres: impact resistant structural composites through damage management. Composites 1990;21:522–30.

[9] Woods DM, Hine PJ, Ward IM. The impact properties of hybrid composites reinforced with high-modulus polyethylene fibres and glass fibres. Compos Sci Technol 1994;52:397–405.

[10] Prevorsek DC, Chin HB, Bhatnagar A. Damage tolerance: design for structural integrity and penetration. Compos Sci Technol 1993;23: 137–48.

[11] Kessler A, Bledzki AK. Low velocity impact behaviour of glass/epoxy cross-ply laminates with different fiber treatments. Polym Compos 1999;20:269–78.

[12] Kim JK, Mai YW. High strength, high fracture toughness fibre composites with interface control — a review. Compos Sci Technol 1991;41:333–78.

[13] Sham ML, Kim JK, Hamada H. Mechanical performance of glass woven fabric laminates: effect of hybrid layers with different silane coupling agents. Polym Compos 1998;6:305–12.

[14] Hirai Y, Hamada H, Kim JK. Impact response of woven glass-fabric composites. I. Effects of fibre surface treatment. Compos Sci Technol 1998;58:91–104.

[15] Hirai Y, Hamada H, Kim JK. Impact response of woven glass-fabric composites. II. Effect of temperature. Compos Sci Technol 1998; 58:119–28.

[16] Caprino G. On the prediction of residual strength of notched laminates. J Mater Sci 1983;18:2269–73.

[17] Sham ML, Kim JK, Wu JS. Interlaminar properties of glass woven fabric composites: mode I and mode II fracture. Key Engng Mater 1998;145–9:799–804.

[18] Bradely WL. Understanding the translation of neat resin toughness into delamination toughness in composites. Key Engng Mater 1989; 37:161–98.

[19] Recker HG, Altstadt V, Eberle W, Folda T, Gerth D, Heckmann W, Ittemann P, Tesch H, Weber T. Toughened thermosets for damage tolerance carbon fibre reinforced composites. SAMPE J 1990;26:73–8.